



Article

A Field Experiment on Wave Forces on an Energy-Absorbing Breakwater

Pasquale G. F. Filianoti ^{1,*}  and Luana Gurnari ² 

¹ Department of Civil, Energy, Environmental and Material Engineering (DICEAM), University “Mediterranea” of Reggio Calabria Via Graziella, 89122 Reggio Calabria, Italy

² Department of Information Engineering, Infrastructure and Sustainable Energy (DIIES), University “Mediterranea” of Reggio Calabria Via Graziella, 89122 Reggio Calabria, Italy; luana.gurnari@unirc.it

* Correspondence: filianoti@unirc.it; Tel.: +39-338-970-6172

Received: 18 January 2020; Accepted: 20 March 2020; Published: 27 March 2020



Abstract: The U-OWC is a caisson breakwater embodying a device for wave energy absorption. Under the wave action, the pressure acting on the upper opening of the vertical duct fluctuates, producing a water discharge alternatively entering/exiting the plant through the U-duct, formed by the duct and the chamber. The interaction between incoming waves and the water discharge alters the wave pressure distribution along the wave-beaten wall of this breakwater compared with the pressure distributions on a vertical pure reflecting wall. As a consequence, the horizontal wave forces produced on the breakwater are also different. A small scale U-OWC breakwater was put off the eastern coast of the Strait of Messina (Southern Italy) to measure the horizontal wave force. Experimental results were compared with Boccotti’s and Goda’s wave pressure formulas, carried out for conventional upright breakwaters, to check their applicability on the U-OWC breakwaters. Both models are suitable for design of U-OWC breakwaters even if they tend to overestimate by up to 25% the actual horizontal loads on the breakwater. Indeed, the greater the absorption of the energy is, the lower the wave pressure on the breakwater wall is.

Keywords: Oscillating Water Column; wave loads; field experiment; pressure distribution; absorption coefficient; caisson breakwater; Goda’s formula

1. Introduction

Vertical breakwaters are structures with a vertical (or nearly vertical) front wall extending from the seabed or based on an artificial foundation. They reflect the incident waves without dissipating much wave energy. The upright section is mostly built with concrete caissons filled with sand, so that the term “caisson breakwater” is often used to indicate such kind of breakwater. The possible modes of major failure of vertical breakwaters by wave actions have been widely investigated by harbor engineers. These are the sliding and overturning of the upright section, geotechnical failure of the foundation and settlement due to the seabed sand being washed away [1–4]. However, from the Japanese experience on breakwaters [1,2], the failures in the foundation occur before the overturning failures.

To verify the stability of these structures, it is necessary to determine the loads exerted by the waves on the front wall. In this regard, several authors proposed valuable models. A pressure formula for standing waves hitting an upright breakwater was introduced by Sainflou (1928) [5]. This model was immediately accepted by engineers for the design of the harbors. In Japan, a method proposed by Hiroi (1919) [6] allows the wave force to be estimated considering the wave pressure as similar to the pressure of a water jet. A formula for breaking wave pressure was proposed by Minikinm (1950) [7], but it has rarely been employed because of the excessive values predicted. Therefore, Ito

et al. (1971) [8] proposed a single formula covering both breaking and non-breaking wave pressures, considering the effects of the presence of a rubble mound foundation. Later, since the 1970s, a new set of formulas concerning the wave pressures on an upright section of a vertical breakwater proposed by Goda [1,9–11], making use of a large volume of laboratory data, has been employed for the design of vertical breakwaters in Japan. An improvement of Goda's method for composite breakwaters was presented by Takahashi et al. (1994) [12]. In the framework of the linear theory of waves, Boccotti (2000) [13] proposed a method for computing the theoretical pressure distribution on a vertical wall. According to this method, the pressure distribution is obtained from the wave pressures measured at the lowest point of the breakwater wall, and assuming that the pressure grows from the bottom up to the surface according to Stokes' first order theory. The wave number is calculated from the wave period of largest waves occurring during a sea storm. To verify the effectiveness of the afore-cited models, a small-scale field experiment on wave forces on upright breakwaters was conducted by Boccotti et al. (2012) [14].

All these models, in particular the models of Boccotti and Goda, are effective for calculating the wave pressure distributions on the front wall of traditional upright breakwaters. U-OWC plants [15–21] are breakwaters in reinforced concrete embodying an Oscillating Water Column (OWC) with a small opening [16]. OWCs are devices for capturing wave energy and consist of a box with a big vertical opening in the front wall, through which waves enter with only some small diffraction effects from the front wall [22], and they propagate on the water surface in the box. A tube, connecting the atmosphere with the air pocket in the plenum chamber, is placed on the roof of the box. This tube contains one or more self-rectifying turbines (e.g., Wells [23]). The air pocket inside the box, alternately, is compressed and expanded. As a consequence, the air flow produced drives the turbine into the tube. Early developments of Oscillating Water Column devices were until 1990. Indeed, Masuda developed a navigation buoy that was the first wave energy device successfully deployed in the sea since 1965. Other concepts for floating OWCs were devised. The Backward Bent Duct Buoy (BBDB) was the main outcome of this concept. It consists in a buoyancy caisson equipped with an L-shaped OWC. In the 1990s, two full-sized fixed OWC plants (on the island of Pico, Azores, Portugal and the island of Islay, Scotland, UK) were realized, both equipped with Wells turbines [24].

U-OWCs belongs to the family of fixed OWCs. They have an additional vertical duct before the wave facing wall of the plenum and extending for the whole caisson width. The upper opening of this duct remains a few meters below the mean water level. Two kinds of U-OWC plants have been widely studied: REWEC1 (Resonant Wave Energy Converter realization n.1) and REWEC3 (Resonant Wave Energy Converter realization n.3). REWEC1 is fully beneath the sea surface, while REWEC3 is partially beneath the sea level and partially above the sea level. In this paper, we deal with REWEC3 breakwaters. Thus, from this point forward, by using the term U-OWC we refer to REWEC3 breakwaters.

As reported by Falcão and Henriques (2016) [24], the first case of a breakwater embodying a wave energy converter into a breakwater was realized in 1990 at the port of Sakata, in Japan. Subsequently, this configuration of a breakwater incorporating an OWC was adopted in Northern Spain, at the port of Mutriku [25]. U-OWC breakwaters are in the early stage, and they have only been built over the last few years. Indeed, a full scale plant of this breakwater has been recently realized in the Civitavecchia Port (Central Italy, Tyrrhenian Sea). It consists of 17 caissons. The absorbing cells are independent with a constant width of 3.87 m [26]. Other projects have been financed in the Marina di Cicerone (Formia, Central Italy) and in the Commercial Port of Salerno (Southern Italy).

The overall stability of a U-OWC device, under the wave actions, can be verified in the same manner as a conventional caisson breakwater, thanks to the structural similarity [27]. Furthermore, due to the absorption of the wave energy of the incoming waves, it is expected that the loads acting on these structures are reduced [28]. Moreover, as reported also by Boccotti [27,29], a novelty in respect to a traditional caisson breakwater is the existence of a vertical force due to the water flow inside the plant that enhances the stability. In addition, as reported by Boccotti (2015) [29], the stability of

conventional OWCs should represent a criticality because of the different geometry in respect to the well-established caisson breakwaters, while that criticality has been overcome by the U-OWC, in which the large experience gained with the design of caisson breakwaters can be used to evaluate the overall stability. Nevertheless, because of the interaction between the incoming waves and the pulsating discharge, which alternatively enters and exits the plant, the main challenge in designing and assessing reliability is predicting the wave loads on the structure. Indeed, the wave pressure distributions on the wave-beaten wall of a U-OWC is different from the pressure distributions on a conventional upright breakwater. Several studies on the wave pressure distribution on the conventional OWC devices have been carried out. The stability of an OWC caisson breakwater was analyzed by Kuo et al. (2015) [30]. They carried out an experiment on a small scale model of an OWC caisson breakwater in a wave flume. They found that the wave pressure on OWC caisson breakwaters is smaller than the wave pressure on a traditional vertical breakwater. Furthermore, the Sainflou's and Goda's formulas were compared with the experimental results, founding an overestimation of the wave pressure on the OWC breakwater and an underestimation in the evaluation of the momentum, respectively. A comparison between the Goda's formula and experimental results on the action of different wave conditions on an OWC in a wave flume was conducted by Ashlin et al. (2017) [31]. These tests revealed that the Goda's formula overestimates the shoreward force and underestimates the seaward force in the range of $d/L < 0.20$. Moreover, Ashlin et al. (2015) [32] analyzed vertical and horizontal wave loads on an OWC, varying the wave frequencies and steepness, observing that at natural frequency of system, the force on the structure is less, due to high-energy absorption by the OWC. There is no similar analysis concerning U-OWC plants.

The aim of this paper is to check the applicability of the Boccotti (first order in the Stokes expansion) and Goda's formulas to calculate the wave pressure distributions on the front wall of a U-OWC. These formulas have been proved valid at predicting the extreme wave pressure distributions in the front wall of traditional upright breakwaters [1,14]. To this purpose, we put directly at sea a small-scale model of a U-OWC breakwater and measured the wave pressure on the wave-beaten wall. The experimental pressure distributions were compared with the wave pressure formula by Boccotti and Goda. In the experiment, the approach of Boccotti (2000) [13] was followed. It is based on the fact that small wind waves can be excellent natural small-scale models of severe sea storms, in the Froude dynamic similarity. This condition is often realized off the eastern coast of the Strait of Messina (Southern Italy), where during certain times of the year several sea states constituted by pure small wind waves can be recorded.

This paper articulates the following:

- general description of U-OWC breakwater and experimental apparatus;
- procedures for calculating experimental and theoretical pressure distributions;
- comparison and discussion of results;
- summary of the work and conclusions.

2. The Small-Scale Model of the U-OWC Breakwater

The U-OWC is also named as REsonant Wave Energy Converter. Under resonant condition, this device is able to capture a significant share of incident wave energy. The absorber breakwater consists essentially of a U-conduit, a branch of which is a vertical duct and the other branch is a box containing an air pocket. The vertical duct is connected with the sea through an upper opening.

A small scale model of a U-OWC has been placed off the beach of Reggio Calabria in the Eastern coast of the Strait of Messina (Southern Italy), with the aim of measuring the extreme wave force on the breakwater. Figure 1 shows the site of the field experiment and the positioning of the device by the pontoon. The location of the experiment is relatively unique in the world, in that there are often pure wind-generated waves with the characteristics (height and period) of a big wave tank.

The “active” part of this model of U-OWC was made of steel, given that the small scale walls were too small to be made of reinforced concrete. Moreover, to simplify manufacturing, the structure was modified from the cellular caisson to the wall in reinforced concrete ballasted with concrete blocks.

The experiment conducted by the authors on the U-OWC breakwaters is analogous to that conducted by Boccotti et al. (2012) [14] on traditional upright breakwaters.



Figure 1. The site of the field experiment (Reggio Calabria, Eastern coast of the strait of Messina) and the positioning of the U-OWC [$38^{\circ}06'32.94''$ N $15^{\circ}38'27.6''$ E].

Figure 2 shows the cross section of the central caisson of both the breakwaters in two different panels. The cross section of the U-OWC breakwater is shown in Figure 2a; the cross section of the upright breakwater in the experiment of Boccotti et al. (2012) [14] is shown in the Figure 2b. As can be seen, the inert part of the U-OWC breakwater was substantially identical to the traditional upright breakwater. In other words, the U-OWC breakwater is the upright breakwater with the addition of the part in steel. Both the cross sections of the central caissons included pressure transducers. In addition, two ultrasonic probes were installed in front of the wave-beaten wall and inside the plenum of the U-OWC breakwater.

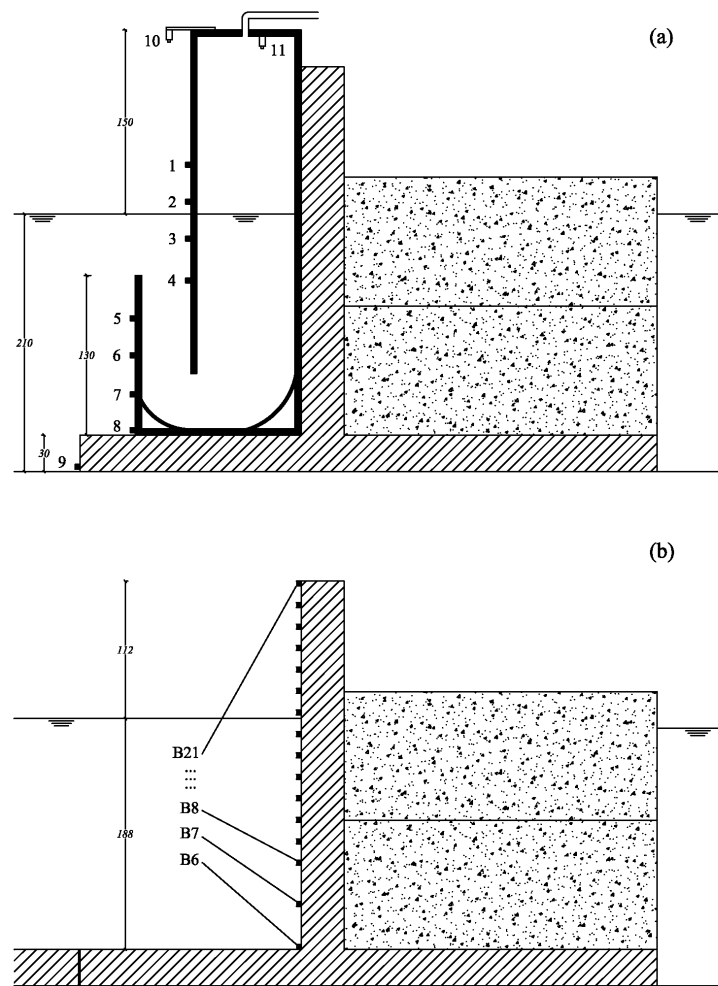


Figure 2. (a) Cross section of the central caisson of the small scale model of U-OWC equipped by gauges (1–9 pressure transducers; 10–11 ultrasonic probes). (b) Cross section of the central caisson of the small scale model of upright breakwater equipped by gauges (from [14]). Measures are in centimeters.

In both experiments, other ultrasonic probes and pressure transducers were supported by two piles located in the undisturbed wave field, in order to measure the incoming waves. The arrangement of the experiment layout is shown in Figure 3.

Both experiments were conducted in the same location. A tiny difference of the mean water levels in front of the breakwaters was recorded, due to the seasonal cycle of tides.

The central caisson of the U-OWC breakwater was placed at 2.1 m depth. The front wall of the central caisson was equipped with a vertical row of nine pressure transducers (each one about 30 cm from the others and from the bottom) allowing the measurement of the horizontal wave force on the breakwater. The ATM/N type pressure transducers, by STS, were used. The range of transducers was [0, 250 mbar] with an accuracy within $\pm 0.25\%$ of FS. For measuring the surface displacement in front of the breakwater, an ultrasonic probe was placed at the top of the vertical wall (Gauge 10 in Figure 2). A second ultrasonic probe was installed inside the plenum to measure the air-water interface vertical displacement (Gauge 11 in Figure 2). To this purpose, we used two IRU-2000 by APG, set to work in the range [0, 3.0 m], with an accuracy of $\pm 0.25\%$ of the detected range. Pressure transducers were numbered from one to nine from the top to the bottom (see Figure 2a). Transducer 9 was placed at the bottom, four transducers (5–8) remain under the upper opening of the vertical duct along the wall around the duct, Transducers 1–3 were placed over the aforesaid opening, along the wall around the plenum, while Transducer 4 was about 2 cm under the the aforesaid opening, along the same wall.

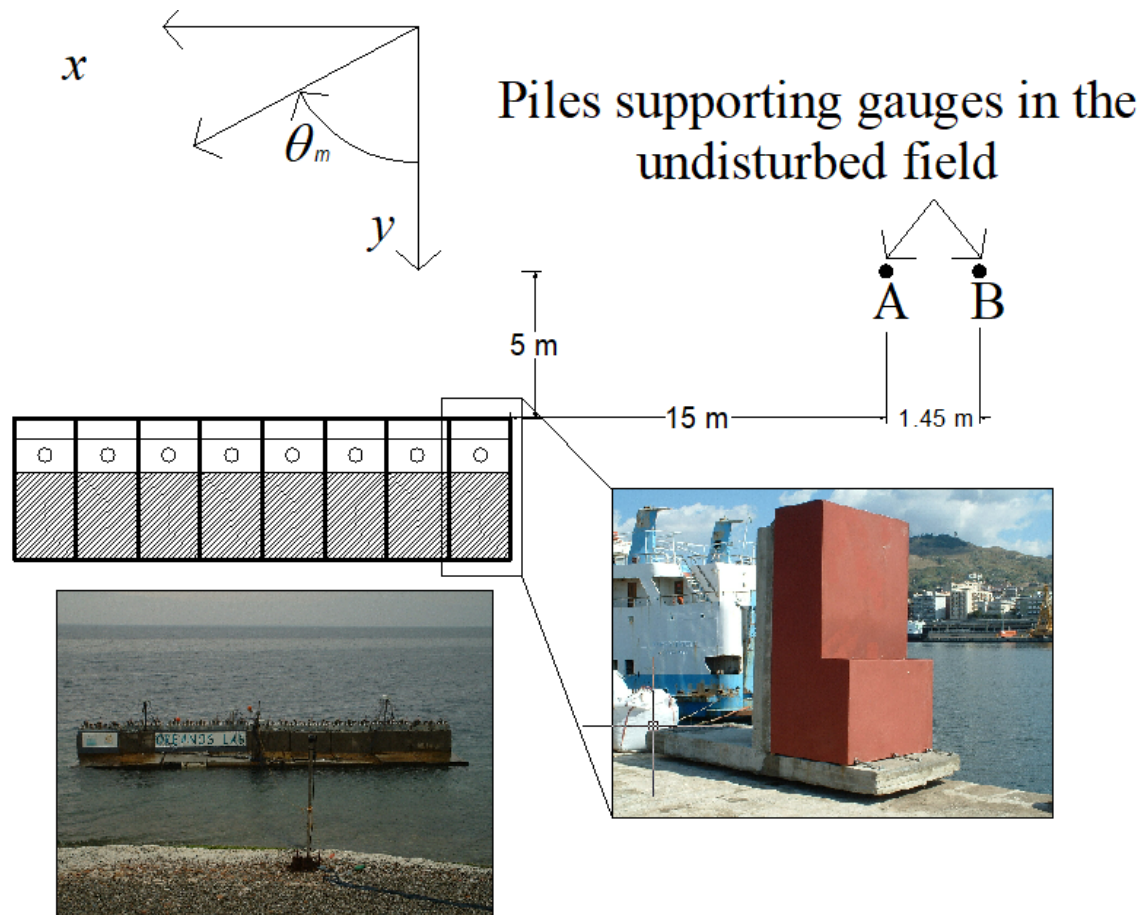


Figure 3. Layout of the experiment at sea.

To calculate surface elevations and wave pressures under the sea level of the incident waves, two ultrasonic probes and two pressure transducers were placed in piles in the undisturbed wave field (see Figure 3).

During the experiment, a set of 774 records of sea states composed by pure wind generated waves (with average peak period of 2.5 s) was obtained. The duration of each record, sufficient to ensure that the process is stationary, was fixed at 5 min. The sampling rate was 10 Hz for each gauge.

An overview of the results is given in Table 1, where all the records are arranged in classes of relative depth d/L_{p0} , variable from 0.15 to 0.30 (the span of each class is 0.05). The mean values of the significant wave height H_s , the peak period T_p , the narrow-bandedness parameter ψ^* [13] and the angle of the wave direction θ_m , are shown to characterize the waves of recorded sea states.

Table 1. Characteristics of the recorded sea states.

d/L_{p0}	<i>N</i> Records	<i>N</i> Waves	H_s (m)	T_p (s)	ψ^*	θ_m
[0.15, 0.20]	206	10,447	0.30	2.8	0.66	0°
[0.20, 0.25]	289	17,793	0.27	2.5	0.64	5°
[0.25, 0.30]	279	21,082	0.25	2.2	0.63	7°

As found by Boccotti et al. (2007) [17], the plant in Figure 2 reaches the maximum absorption when the period of the incoming waves is close to 3.5 s (eigenperiod of the plant).

3. Experimental Pressure Distribution on the Small-Scale Model of the U-OWC

The ratio $\tilde{F}(t)$ between the effective force $F(t)$ on the wall and its standard deviation σ_F was calculated for each recorded sea state. The positive peaks of the process $\tilde{F}(t)$ were identified and classified in order of height: the first is the highest peak, the last is the smallest peak. The pressure distributions below crests, obtained through the instantaneous values of pressure recorded by the transducers placed along the vertical row in front of the central caisson (Gauges 1–9 presented in Figure 2a), were stored in the time instant when each positive peak value of $\tilde{F}(t)$ occurred.

Figure 4 shows a 20-s record of the pressure measured by transducers 1–9 and the corresponding wave force $F(t)$. This time plot is a part of 5 min record of a sea state of pure wind waves. In the same figure, the amplitudes of the positive and negative peaks of $F(t)$ and the corresponding amplitudes of the pressure head waves are represented by dotted lines. All similar records, obtained during the experiment, represent input data for calculating the pressure distributions. Each pressure distribution p_{wi} ($i = 1, 2, \dots, 9$) was divided by the standard deviation σ_{pwb} of the wave pressure at the base (measured by Gauge 9) and stored as a function of the relative quotes ξ_i/d . The quote ξ_i of each transducer, measured upwards from the bottom, did not change during the experiment, whereas the depth d generally changed in each record owing to the variation of the tide.

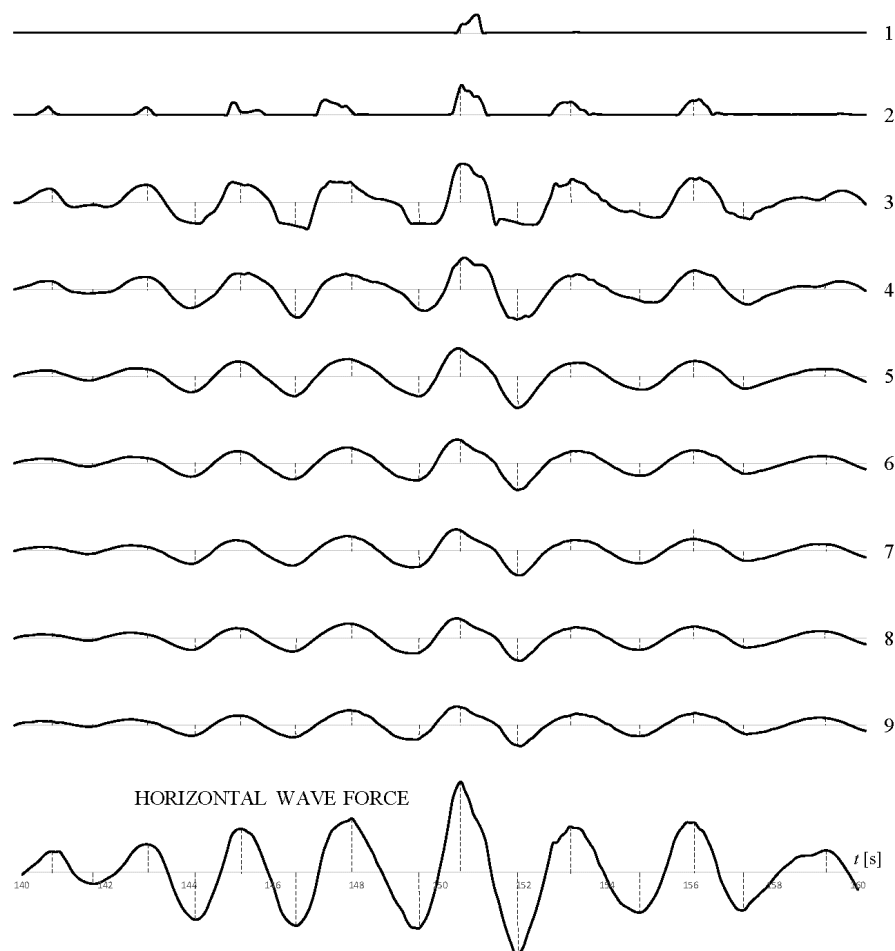


Figure 4. Wave pressure p_{wi} , recorded at various depths on the central caisson of the U-OWC breakwater (see Figure 2a for the gauge map), and the horizontal force obtained by integrating the p_{wi} along the front wall of the breakwater.

The 1/10, 1/100 and 1/1000 wave distributions of the highest positive peaks of the process $\tilde{F}(t)$ were calculated, and the related mean pressure distributions on the front wall were obtained.

The 1/10, 1/100 and 1/1000 pressure distributions of the crests were calculated for each range of relative depth assumed in Table 1. The 1/ N pressure distribution represents the distribution of the mean values of the wave pressures corresponding to the n/N highest positive peak values of $\tilde{F}(t)$, where n is the number of waves of the $\tilde{F}(t)$ process in the fixed interval.

The same procedure was carried out for the highest negative peaks (troughs) of the process $\tilde{F}(t)$, therefore the related mean pressure distributions 1/10, 1/100 and 1/1000 were obtained.

4. Wave Pressure on a Vertical Wall: Goda's and Boccotti's Formulas

Wave pressure formulas for the design of vertical upright breakwaters have been proposed, among others, by Boccotti (2000) [13] and Goda (1992) [10]. Boccotti pointed out that the pressure distributions on a vertical wall are close to the distributions obtained from linear wave theory (first order in the Stokes expansion). Goda carried out some formulas to determine the extreme wave pressure under wave crests, assuming the existence of a trapezoidal pressure distribution along a vertical wall.

According to the linear wave theory, the largest positive pressures and the largest negative pressures can be calculated by means of the following equations:

(a) Wave crest:

$$P_w \begin{cases} = \rho g H^{(+)} \frac{\cosh(k\zeta)}{\cosh(kd)} & \text{if } 0 \leq \zeta \leq d, \\ = \rho g (d + H^{(+)} - \zeta) & \text{if } d \leq \zeta \leq d + H^{(+)}, \end{cases} \quad (1)$$

(b) Wave trough:

$$P_w \begin{cases} = \rho g H^{(-)} \frac{\cosh(k\zeta)}{\cosh(kd)} & \text{if } p_w > -p_{st}, \\ = -p_{st} & \text{otherwise,} \end{cases} \quad (2)$$

where ζ is the vertical coordinate with origin at the lowest point of the front wall, p_{st} is the hydrostatic pressure, and $H^{(+)}$ and $H^{(-)}$ are the virtual wave height, under a crest and under a trough, respectively, which can be evaluated by means of

$$H^{(+)} = \frac{1}{\rho g} p_{wb}^{(+)} \cosh(kd), \quad (3)$$

$$H^{(-)} = \frac{1}{\rho g} p_{wb}^{(-)} \cosh(kd), \quad (4)$$

where $p_{wb}^{(+)}$ and $p_{wb}^{(-)}$ are measured at the lowest point of the front wall, respectively, at the instant time of the wave crest and at the instant time of the wave trough. According to Boccotti's model, the pressure distributions on a vertical wall are close to the distributions obtained from the theory of the linear wave (Equations (1) and (2)), in which the wave number k is calculated by the wave period T_h on the water depth d . T_h is the period of the highest wave in the design sea state, according to the quasi-determinism theory [13] (T_h is very close to $T_{1/3}$ used by Goda). For a very large wave with respect to the average of a given sea state, the positive pressures are typically smaller than the negative pressures.

The virtual heights $H^{(+)}$ and $H^{(-)}$ in Boccotti's formula are reproduced in Table 2. They are obtained as results of a small scale experiment, in which wave pressure is generated by the wind waves ($0.15 < d/L_{p0} < 0.20$) hitting a vertical wall (see Figure 13.4 and Section 13.1.4 in [13]). To estimate $H^{(+)}$ and $H^{(-)}$, a simple relation between the standard deviation σ_{pwb} of the wave pressure at the base of the wall and the standard deviation σ of the surface wave in the undisturbed wave field ($\sigma = 4H_s$) was suggested by Boccotti (2000) [13]:

$$\frac{\sigma_{pwb}}{\sigma} = \frac{2\rho g}{\cosh(kd)}. \quad (5)$$

Table 2. Virtual wave heights $H^{(+)}$ and $H^{(-)}$ on a vertical wall ([14]).

	$H^{(+)} / H_s$	$H^{(-)} / H_s$
$F_{1/10}$	1.00	1.50
$F_{1/100}$	1.24	2.03
$F_{1/1000}$	1.40	2.31

An alternative approach to estimate the wave pressure distributions on a vertical wall was proposed by Goda (1992) [10]. The pressure distribution according to Goda's formula is shown in Figure 5.

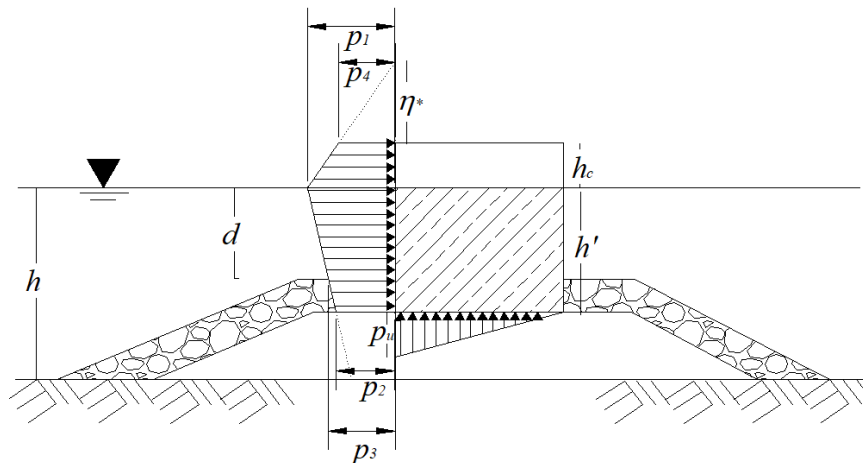


Figure 5. Distribution of wave pressure on an upright section of a vertical breakwater according to the model of Goda (from Goda, 2010). Values are referred to the mean.

There, h represents the water depth in front of the breakwater and h' is the distance between the design water level and the bottom of the upright section. The depth above the armor layer of the rubble foundation is d , and h_c is the crest elevation of the breakwater above the still water level. The highest wave is taken as $H_{max} = 1.8H_{1/3}$ seaward of the surf zone, while, within the surf zone, the highest of random breaking waves H_{max} at the distance $5H_{1/3}$ seaward of the breakwater is taken as the wave height. The period of the largest wave is taken equal to $T_{1/3}$ ($H_{1/3}$ is the mean wave height of the 1/3 largest waves in the sea state, while $T_{1/3}$ is the mean period of the above cited waves).

The maximum wave elevation in the breakwater center and the pressure intensities are to be estimated as below:

$$\eta^* = 0.75(1 + \lambda_1 \cos \theta) H_{max}, \quad (6)$$

$$p_1 = \frac{1}{2}(1 + \cos \theta)(\alpha_1 \lambda_1 + \alpha_2 \lambda_2 \cos^2 \theta) \rho g H_{max}, \quad (7)$$

$$p_2 = \frac{p_1}{\cosh(2\pi h/L)}, \quad (8)$$

$$p_3 = \alpha_3 p_1, \quad (9)$$

where p_1 is the wave pressure at the still water level, p_2 represents the wave pressure at the bottom depth, p_3 is the wave pressure at the depth of the base of the armor layer and, finally, p_4 represents the wave pressure at the structure crest, that it is determined by linearly interpolating between p_1

and η^* . Therefore, θ denotes the angle between the direction of the wave and the line normal to the breakwater, and

$$\alpha_1 = 0.6 + \frac{1}{2} \left[\frac{4\pi h/L}{\sinh(4\pi h/L)} \right]^2, \quad (10)$$

$$\alpha_2 = \min \left\{ \frac{h_b - d}{3h_b} \left(\frac{H_{max}}{d} \right)^2, \frac{2d}{h_{max}} \right\}, \quad (11)$$

$$\alpha_3 = 1 - \frac{h'}{h} \left[1 - \frac{1}{\cosh(2\pi h/L)} \right], \quad (12)$$

where $\min\{a, b\}$ refers to the smaller one between a or b , and h_b is the water depth at the distance $5H_{1/3}$ seaward of the breakwater. The uplift pressure p_u is

$$p_u = \frac{1}{2} (1 + \cos\theta) \alpha_1 \alpha_2 \lambda_3 \rho g H_{max}. \quad (13)$$

For breakwaters having simple upright sections, factors λ_1 , λ_2 and λ_3 are set equal to 1. Goda does not give a formula for negative wave pressures (pressures under wave troughs).

5. Comparison between Models and the Actual Pressure Distributions

In this Section, the actual pressure distributions on the front wall of the U-OWC are compared with those obtained by means of the two models described in the previous Section. The average of the pressure distributions produced by the $n/10$, $n/100$ and $n/1000$ highest crests and by the $n/10$, $n/100$ and $n/1000$ deepest troughs of the force process were calculated in three range of d/L_{p0} : [0.15, 0.20], [0.20, 0.25], [0.25, 0.30]; where n is the number of waves recorded during the small scale field experiment. Both the models were conceived for use with long traditional upright breakwaters whose C_D is equal to 2 ($C_D \equiv$ significant wave height in front of the breakwater/significant wave height in the undisturbed wave field). Here, in the application of the two models, we take into account the actual values of C_D calculated in presence of the U-OWC breakwater during the experiment. These values are calculated as the ratio between the standard deviation of the sea states in front of the breakwater σ_{re} , recorded by an ultrasonic probe (see Figure 2, Gauge 10), and the standard deviation of the surface waves in the undisturbed wave field σ_{in} , measured by ultrasonic probes in two piles far from the breakwater (see Figure 3). These ratios are generally different in respect to the well-known values in front of a pure reflective breakwater, because of the wave energy captured by the U-OWC which generally involves lower values of σ_{re} .

The measured ratios $p_{wb}^{(+)} / \sigma_{pwb}$ and $p_{wb}^{(-)} / \sigma_{pwb}$ and the corresponding mean values \bar{C}_D are reproduced for the distributions $F_{1/10}$, $F_{1/100}$ and $F_{1/1000}$ for each of the three class of for each class of d/L_{p0} aforesaid. As we can see, the dimensionless pressure values at the base of the breakwater and the mean values of the diffraction coefficient in front of the U-OWC, grow to the growth of n in the $F_{1/n}$ distributions. Moreover, \bar{C}_D always results less than 2, except in the case of crests distributions $F_{1/1000}$, in the interval $0.25 < d/L_{p0} < 0.30$, where it is equal to 2.28.

With Goda's formula for wave estimation, we have found $H_{1/3} = H_s$ and $T_{1/3} = T_h$, so that they can be compared with 1/1000 distributions.

In Figure 6, the average of the 1/10, 1/100 and 1/1000 pressure distributions of crests and troughs is represented in the range of d/L_{p0} [0.15, 0.20], [0.20, 0.25], [0.25, 0.30]. Points are the measured pressures on the front wall of the U-OWC, continuous lines are pressure distributions from the Boccotti's model (Equations (1)–(4)), dotted lines are pressure distributions from the Goda's formula (Equations (6)–(13)).

The linear wave distribution utilized by Boccotti, agrees well with the experimental data for the troughs in the ranges [0.15, 0.20] and [0.20, 0.25] of d/L_{p0} . A 20% overestimation relative to the experimental data can be observed for 1/1000 troughs distribution in the range [0.25, 0.30] of d/L_{p0} .

In the same range of d/L_{p0} , the linear wave distribution of the crests overestimates experimental data in proximity of the mean water level, whereas it slightly underestimates them in the range $[0.20, 0.25]$ of d/L_{p0} .

Goda's model generally overestimates the pressure distributions in all considered intervals, mainly for d/L_{p0} in the range $[0.20, 0.25]$.

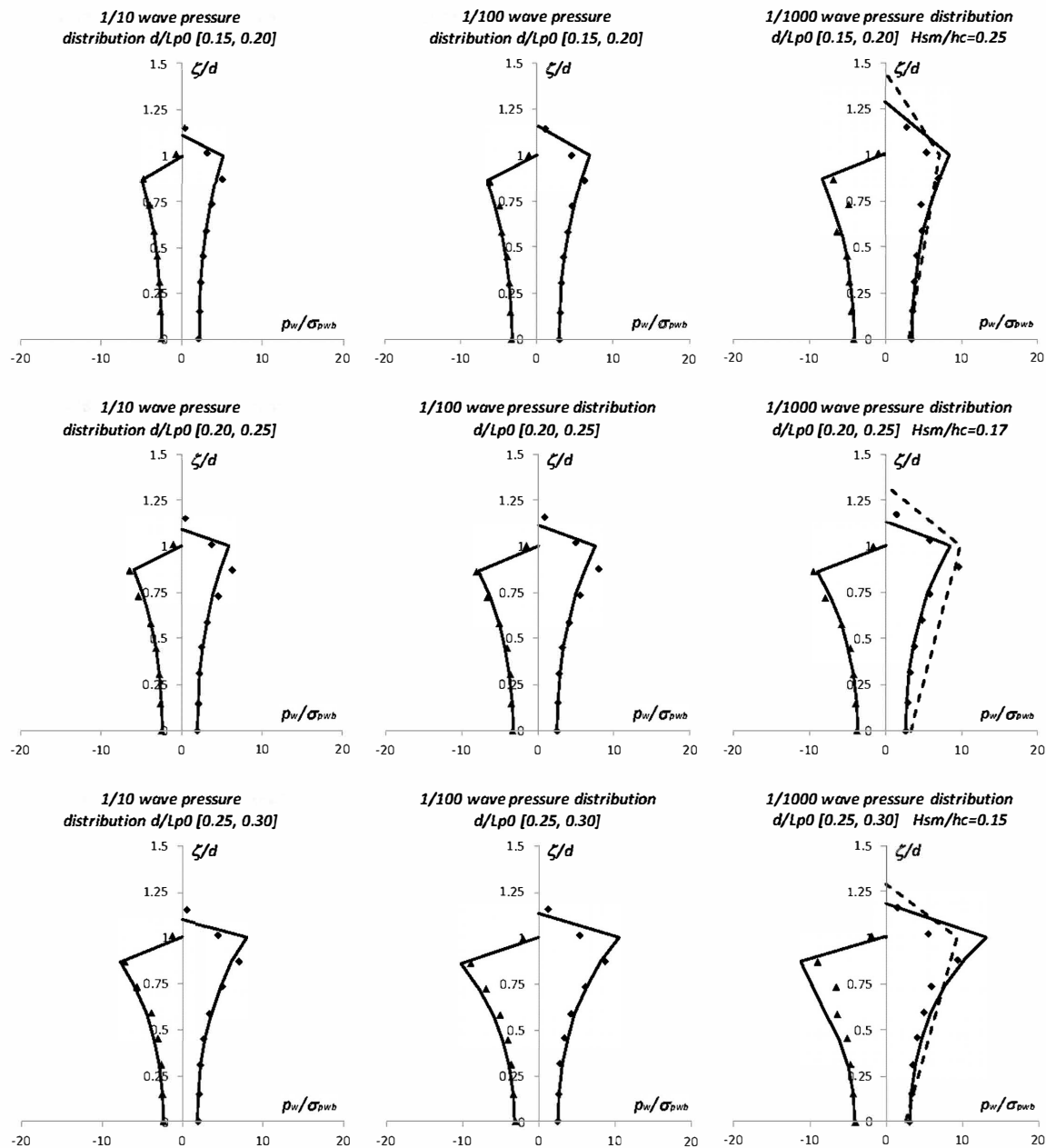


Figure 6. Average of the highest 1/10, 1/100 and 1/1000 wave pressure distribution (crests and troughs) of sea states constituted by wind waves in fixed intervals of d/L_{p0} (see Table 1). Points represents experimental results, the continuous lines and the dotted line represent the pressure distribution obtained by means of Boccotti's and Goda's formulas, respectively.

6. Why Is the Actual Pressure Distribution on a U-OWC Breakwater in Proximity of the Mean Sea Level Different from that Obtained from the Linear Wave Model?

In the previous section, we point out that the linear wave pressure distributions significantly deviate from the measured values, in the portion of the wave-beaten wall lying between the upper

opening of the vertical duct and the mean water level. In other words, some second-order effects are realized in this region, probably due to the alternating vertical water flux produced by waves hitting the wall.

As a result of their experiment conducted on a U-OWC breakwater, Boccotti et al. (2007) [17] concluded that a breakwater embodying a wave energy converter can absorb a considerable share of wave energy, thanks to a great amplification of the wave height.

In this study, we found confirmation of some huge amplification of the frequency spectrum in front of the breakwater, in comparison with the frequency spectrum in the undisturbed wave field. The comparison can be carried out by means of pieces of spectrum (POS) in fixed frequency domains. In particular, we can define

$$\beta \equiv \frac{1}{2} \sqrt{\int_{f_1}^{f_2} E_w(f) df / \int_{f_1}^{f_2} E_u(f) df} \quad (14)$$

where E_w and E_u are, respectively, the energy spectrum measured on the wave-beaten wall over the upper opening of the vertical duct, and the energy spectrum measured in the undisturbed wave field, at the same depth and f is the natural frequency. Values of β equal to 1 in all pieces of spectrum means that the breakwater behaves as a pure reflective wall (an infinitely long vertical wall, non-absorbing breakwater). Values of β greater than 1 are indices of a larger amplification of waves in front of the breakwater with respect to a pure reflecting breakwater, and conversely in the case of β less than 1.

In the case of U-OWC breakwaters, not only is β generally different from 1, but β varies among different pieces of spectrum in the same spectrum. In particular, in many sea states, we observed a huge amplification of the piece of spectrum corresponding to the lowest frequencies with respect to the amplification of the piece of spectrum corresponding to the peak frequencies measured in the undisturbed wave field.

These remarks are confirmed in Figure 7, in which some energy spectra E_w and E_u , obtained from the registrations during the experiment on the U-OWC breakwater, are represented for different wave conditions. In particular, each panel shows comparisons between the spectrum of the pressure fluctuations recorded by the transducer placed in front of the breakwater, on the upper opening of the vertical duct, and the spectrum of the pressure fluctuations recorded by the transducers in the undisturbed wave field, placed at the same depth beneath the mean water level.

Moreover, a summary table, reproducing the pieces of spectrum and the corresponding values of β , is reported for each sea state. In each panel, three pieces of spectrum have been identified. The central piece (second) is that in which the peak has been detected, so that it contains the highest energy part.

Figure 7a–c shows the frequency spectra corresponding to sea states for which huge amplifications have been observed. In all of these three cases the value of β corresponding to the second POS is greater than one. This is in accordance with the measured diffraction coefficient of the surface waves, which result greater than 2 (it is variable from 2.1 to 2.2). In other words, the wave in front of the U-OWC in Cases (a)–(c) is higher than that which can be measured on a pure reflective wall. More high values of β have been measured in the first POS. This means that the amplification of the spectra corresponding to the lowest frequencies is greater than that corresponding to the frequencies around the value of the peak frequency in the undisturbed wave field (incident waves). As a consequence, as we can see, the spectra in front of the U-OWC present in general two peaks: the highest corresponding to a frequency very close to the peak frequency of the incident waves, the other, corresponding to a lower frequency, in which the values of the energy spectrum in the undisturbed wave field are negligible. Figure 7d shows the spectra corresponding to a recorded sea state whose synthesis parameters are well representative of the average of all recorded sea states, constituted by wind waves. In this case, the values of β in all POS are less than 1. According to these values of β , the diffraction coefficient of the surface waves measured in front of the U-OWC is about 1.85. In this case as well, a significant amplification of the spectrum corresponding to the lowest frequencies appears, whereas a huge peak

(although lower than those emerging in Figure 7a–c) remains in correspondence to the peak frequency in the undisturbed wave field.

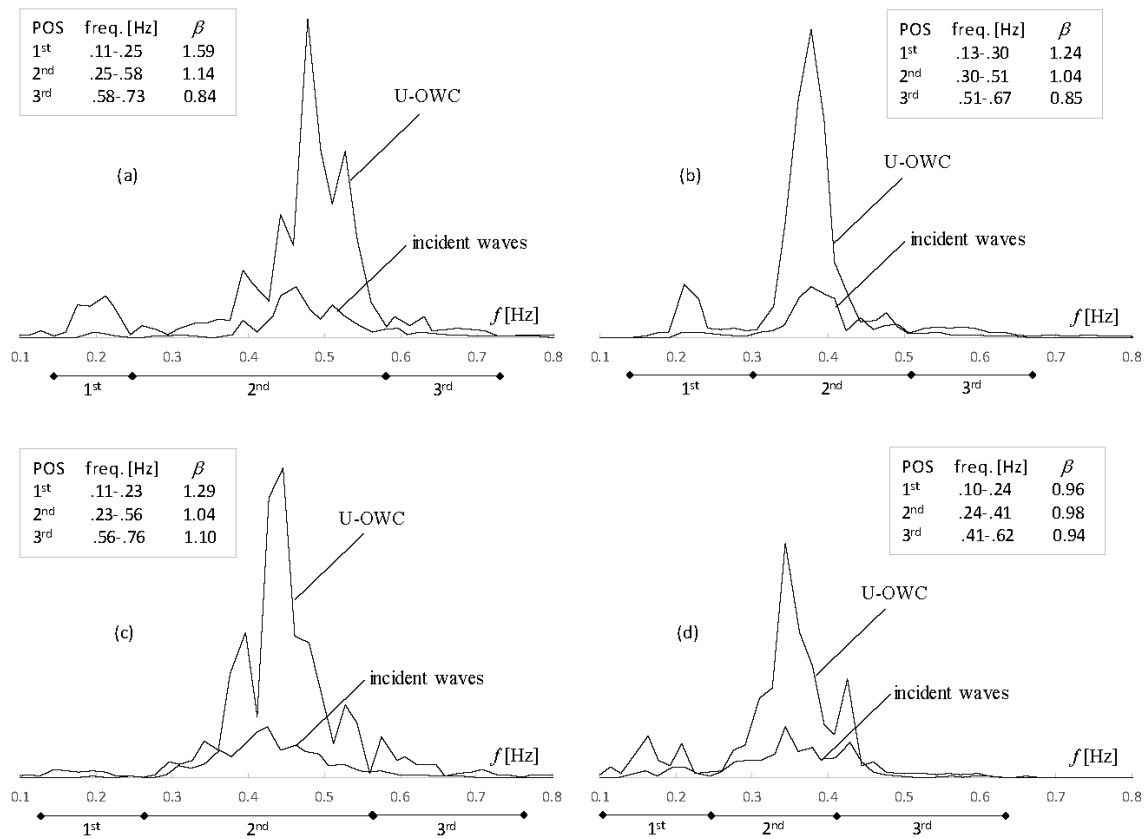


Figure 7. Frequency spectra of the pressure fluctuations recorded at the upper opening of the vertical duct and in the undisturbed wave field. For each sea state some values of the amplification factor β of piece of spectrum are reported. In Registration (a), 25% of absorption of the whole incident energy has been measured; 81% in Registration (b); 42% in Registration (c); and 52% in Registration (d).

Therefore, the variation of β with the frequency of the spectrum, and in particular the amplification of the lowest frequencies, alters the shape of the spectrum on the upper opening of the vertical duct, in comparison with the shape of the spectrum of the incident waves. This explains the relative deviation of the measured wave pressure distributions from the linear theoretical model in the portion of the wave-beaten wall of the U-OWC, lying between the upper opening of the vertical duct and the mean water level. In other words, in this area, non-linear effects, due to the alternating vertical water flux inside the plant, which is produced by waves hitting the wall, are considerable. Nevertheless, the next Sections show that the linear wave theory, however, is able to predict, with an appropriate safety level, the extreme wave force on a U-OWC breakwater.

7. The Virtual Wave Heights in Front of a U-OWC Breakwater

The virtual wave heights $H^{(+)}$ and $H^{(-)}$ in front of a U-OWC breakwater can be calculated taking in account that the diffraction coefficient is generally different by 2, as seen in the previous Section. Therefore, Equations (3) and (4) for a U-OWC breakwater can be written, respectively, in the form:

$$H^{(+)} = \frac{\bar{C}_D}{2\rho g} p_{wb}^{(+)} \cosh(kd), \quad (15)$$

$$H^{(-)} = \frac{\bar{C}_D}{2\rho g} p_{wb}^{(-)} \cosh(kd). \quad (16)$$

Making use of the Equation (5), we obtain:

$$\frac{H^{(+)}}{H_s} = \bar{C}_D \frac{p_{wb}^{(+)}}{\sigma_{pwb}}, \quad (17)$$

$$\frac{H^{(-)}}{H_s} = \bar{C}_D \frac{p_{wb}^{(-)}}{\sigma_{pwb}}, \quad (18)$$

where \bar{C}_D , $p_{wb}^{(+)}/\sigma_{pwb}$ and $p_{wb}^{(-)}/\sigma_{pwb}$, correspondent to 1/10, 1/100 and 1/1000 force process distributions, were calculated for each class of d/L_{p0} , as reported in Table 3.

Table 3. Pressure distributions at the base of the U-OWC breakwater and mean values of the diffraction coefficient in front of the U-OWC corresponding to 1/10, 1/100 and 1/1000 force process in fixed intervals of d/L_{p0} .

d/L_{p0}	Force Distributions	Crests		Troughs	
		$p_{wb}^{(+)}/\sigma_{pwb}$	\bar{C}_D	$p_{wb}^{(-)}/\sigma_{pwb}$	\bar{C}_D
[0.15, 0.20]	$F_{1/10}$	2.1	1.73	−2.5	1.75
	$F_{1/100}$	2.9	1.70	−3.3	1.76
	$F_{1/1000}$	3.5	1.83	−4.1	1.77
[0.20, 0.25]	$F_{1/10}$	2.0	1.81	−2.4	1.82
	$F_{1/100}$	2.5	1.82	−3.2	1.80
	$F_{1/1000}$	2.6	1.86	−3.7	1.81
[0.25, 0.30]	$F_{1/10}$	1.9	1.88	−2.4	1.88
	$F_{1/100}$	2.5	1.86	−3.2	1.94
	$F_{1/1000}$	3.1	2.28	−4.1	1.97

Thus, a set of virtual height values, $H^{(+)}$, $H^{(-)}$, in front of a U-OWC breakwater, for the same interval of d/L_{p0} considered by Boccotti et al. (2012) [14] (for a conventional breakwater, see Table 2), is shown in Table 4. For comparison, it emerges that the 1/1000 force process in front of the U-OWC is nearly 15% greater than that in front of an upright breakwater, whereas the one which corresponds to the 1/10 force process is nearly 10% lower. For the 1/100 force distribution, the $H^{(+)}$ values are almost identical. Regarding the trough distributions, $H^{(-)}$ values in front of a U-OWC are on average 25% lower than the corresponding ones in front of an upright breakwater. In particular, the average pressure distribution of the greatest ($n/1000$) positive force peaks (n being the total number of waves) is expected to be very close to the pressure distribution under the wave crest of a periodic wave with a height of $1.60H_s$ and a period of T_h . This distribution is the most important because it can be assumed for design purposes, given that the design sea state typically contains a few thousand waves. Similarly, the average pressure distributions of the greatest ($n/1000$) negative force peaks are expected to be very close to the pressure distributions under the wave trough for a periodic wave with a height of $1.81H_s$ and a period of T_h .

8. Wave Forces on a U-OWC: Comparison between Models and Experimental Results

The extreme horizontal wave forces on the U-OWC breakwater can be calculated by integrating the instantaneous wave pressure distributions along the front wall.

The effectiveness of the models previous described to predict the wave action on the U-OWC breakwater is estimated by means of two indices:

$$\Delta_{B1/N} = 100 \frac{|F_{B1/N}| - |F_{1/N}|}{|F_{1/N}|}, \quad (19)$$

and

$$\Delta_G = 100 \frac{|F_G| - |F_{1/1000}|}{|F_{1/1000}|}, \quad (20)$$

where $F_{1/N}$ is the actual horizontal wave force (calculated from measured pressures), $F_{B1/N}$ is the horizontal wave force calculated by Boccotti's model, and F_G is the horizontal wave force calculated with Goda's formula. The wave forces, calculated according to the Boccotti's model, have been obtained by integrating Equations (1) and (2) along the front wall, using the values of $H^{(+)}$ and $H^{(-)}$ obtained during the experiment, and reproduced in Table 4.

Table 4. Virtual wave heights $H^{(+)}$ and $H^{(-)}$ in front of a U-OWC, in the interval $0.15 < d/L_{p0} < 0.20$.

	$H^{(+)}/H_s$	$H^{(-)}/H_s$
$F_{1/10}$	0.91	1.09
$F_{1/100}$	1.23	1.45
$F_{1/1000}$	1.60	1.81

The percentage differences $\Delta_{B1/N}$ and Δ_G are given in Table 5, for the case of the positive force, and, in Table 6, for the case of the negative force.

Table 5. Positive force peaks: percentage difference between models and measured extreme horizontal forces on the U-OWC ($\Delta_{B1/N}$ are calculated from $H^{(+)}$ values in Table 4).

d/L_{p0}	$\Delta_{B1/10}$	$\Delta_{B1/100}$	$\Delta_{B1/1000}$	Δ_G
[0.15, 0.20]	−2.0	+3.9	+12.3	+10.0
[0.20, 0.25]	0.0	+9.2	+17.3	+35.1
[0.25, 0.30]	+20.9	+35.7	+40.7	+39.6

Table 6. Negative force peaks: percentage difference between Boccotti's model and measured extreme horizontal forces on the U-OWC ($\Delta_{B1/N}$ are calculated from $H^{(-)}$ values in Table 4).

d/L_{p0}	$\Delta_{B1/10}$	$\Delta_{B1/100}$	$\Delta_{B1/1000}$	Δ_G
[0.15, 0.20]	−4.4	−4.2	−3.7	-
[0.20, 0.25]	−6.6	−7.1	−1.4	-
[0.25, 0.30]	+2.2	+1.0	+3.5	-

As we can see, the Boccotti's model predicts the extreme positive force peaks on a U-OWC breakwater, with an average overestimation of 23%. In particular, this model overestimates the positive force peaks corresponding to the 1/1000 distribution of about 12% in the range [0.15, 0.20] of d/L_{p0} , 17% in the range [0.20, 0.25], and 41% in the range [0.25, 0.30]. The overestimation of the positive force peaks corresponding to the other distribution is lower. The Boccotti's model overestimates the positive force peaks corresponding to the 1/100 distribution of about 4% in the range [0.15, 0.20], 9% in the range [0.20, 0.25], and 35% in the range [0.25, 0.30], whereas it overestimates the positive force peaks corresponding to the 1/10 distribution of about 21% in the range [0.25, 0.30]. The positive force peaks corresponding to the 1/10 distribution in the other ranges of d/L_{p0} are substantially identical.

In addition, the Goda distribution overestimates the positive force peaks on a U-OWC breakwater. In comparison to the 1/1000 distributions obtained by means of the Boccotti's model, the overestimation of the actual values is similar in the ranges [0.15, 0.20] and [0.25, 0.30], whereas it is about twice in the range [0.20, 0.25]. In summary, the average overestimation of the actual values is 28%, by means of Goda's model.

Thus, we can conclude that both the models predict the extreme positive force peaks on a U-OWC breakwater with an appropriate safety factor. Regarding to the extreme negative force peaks on a U-OWC breakwater, they are underestimated by Boccotti's model in the range [0.15, 0.20] and [0.20, 0.25], whereas they are overestimated in the range [0.25, 0.30]. Nevertheless, these are small values, as the maximum underestimation is about 4% in the range [0.15, 0.20] and 7% in the range [0.20, 0.25], whereas the maximum overestimation is about 4% in the range [0.25, 0.30]. Thus, we can observe that the prediction of the negative force peaks is more accurate than the positive force peaks, and in particular in the 1/1000 force peaks distributions which are very important because they are generally considered for design purposes.

The Boccotti's model, applied with the virtual wave heights $H^{(+)}$ and $H^{(-)}$ obtained in front of a vertical wall (see Table 2) and used in [14] to predict the extreme force peaks on conventional upright breakwaters, underestimates the positive force peaks in front of a U-OWC breakwater by about 11% in the range [0.15, 0.20] and about 7% in the range [0.20, 0.25], whereas it overestimates them by about 15% in the range [0.25, 0.30]. All the negative force peaks are overestimated from a minimum of 10% to about 25%.

The Boccotti's model underestimates both positive and negative extreme force peaks in front of an upright breakwater. The underestimation of the positive force peaks is lower than 7%, whereas it can reach almost 20% for the negative force peaks (see 1/1000 distributions in [14]). Therefore, the wave forces on a U-OWC breakwater are generally smaller than ones on a conventional upright breakwater.

9. Pressure Distribution as a Function of the Energy Absorbed by the Plant

Pressure distributions shown in Figure 6 were calculated at the front wall of the U-OWC breakwater regardless the energy captured by the plant is. Indeed, each record, considered in the previous Section was taken during plant working, represented a sea state with the plant working (i.e., absorbing the wave energy). Figures 8 and 9 show the instantaneous wave pressure fluctuation and water discharge on the outer opening of the plant and the energy flux absorbed by the U-OWC, respectively.

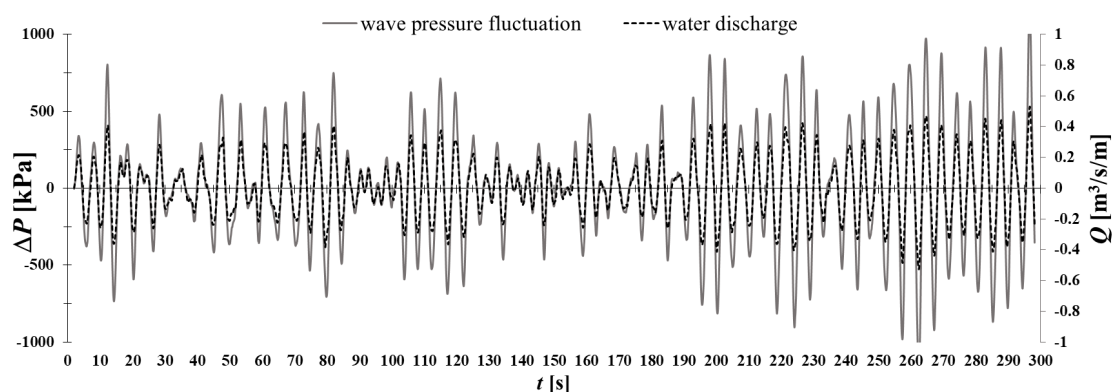


Figure 8. A 300s time history of the instantaneous wave pressure fluctuation and water discharge on the outer opening of the plant.

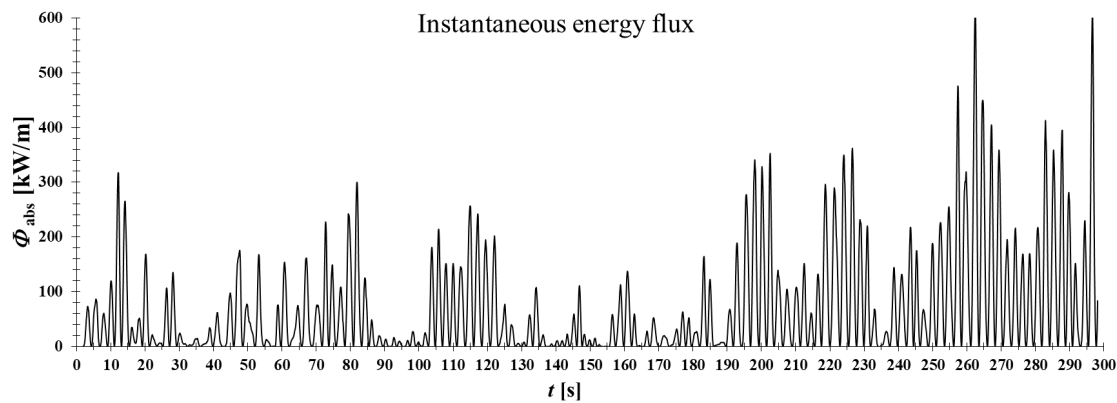


Figure 9. The instantaneous energy flux absorbed by the U-OWC, during the same time intervals shown in Figure 8.

In particular, the instantaneous energy flux Φ_{abs} , shown in Figure 9, was evaluated by multiplying the pressure fluctuation $\Delta P(t)$ by the pulsating discharge $Q(t)$, shown in Figure 8. The method to obtain the water discharge $Q(t)$ is illustrated in [33]. The absorption coefficient C_A is the ratio between the time-average energy flux absorbed by the plant $\bar{\Phi}_{abs}$, and the time-average energy flux of the incoming waves $\bar{\Phi}_{in}$, evaluated in the undisturbed field. The latter was obtained by the method illustrated in [17], starting from the pressure recorded by transducers supported by the two piles A and B, shown in Figure 3.

To evaluate the effects of the energy absorbed by the plant on wave forces, the wave pressure distributions for the records falling in the range $0.15 < d/L_{p0} < 0.20$ were classified into four intervals of C_A : [0, 25%], [25%, 50%], [50%, 75%] and [75%, 100%], the results of which are shown in Figure 10. Distributions relevant to $F_{1/1000}$, for $0 < C_A < 0.75$ are not present, in that they are not meaningful, because of the lack of enough recorded data in the given interval. The three wave pressure distributions in the upper row are for $0 < C_A < 100$ (therefore, they are the same as in Figure 6). As we can see, the linear wave theory tends to slightly underestimate the wave forces in correspondence of the lowest values of C_A (i.e., in the range [0, 25%]), for $F_{1/10}$ and $F_{1/100}$. This underestimation is more evident during troughs. The more the C_A increases, the more the linear wave theory tends to underestimate the actual wave pressure and, consequently, the wave forces. This is due to an evident drop of the wave pressure in proximity to the outer opening of the vertical duct, as we can see in the distribution at the lower right corner of Figure 10. The pressure energy is partly spent to feed the large eddy near the opening (see Figure 13 of [34]) and is partly converted into velocity of the water entering the plant.

As regards the 1/1000 distribution, which is the most relevant because it is generally assumed for design purposes, the linear wave theory overestimates the horizontal wave force on the front wall of the U-OWC by about 18%, whereas it underestimates the same force on a upright breakwater by about 5% [14]. As a consequence, the extreme wave force on a U-OWC is almost 23% smaller than the extreme wave force on a traditional upright breakwater. The linear wave theory also overestimates by the same quantity the overturning moment due to the horizontal wave force, while the uplift force is the same, because the actual wave pressure at the base of the breakwater is taken as an input in the Boccotti's model.

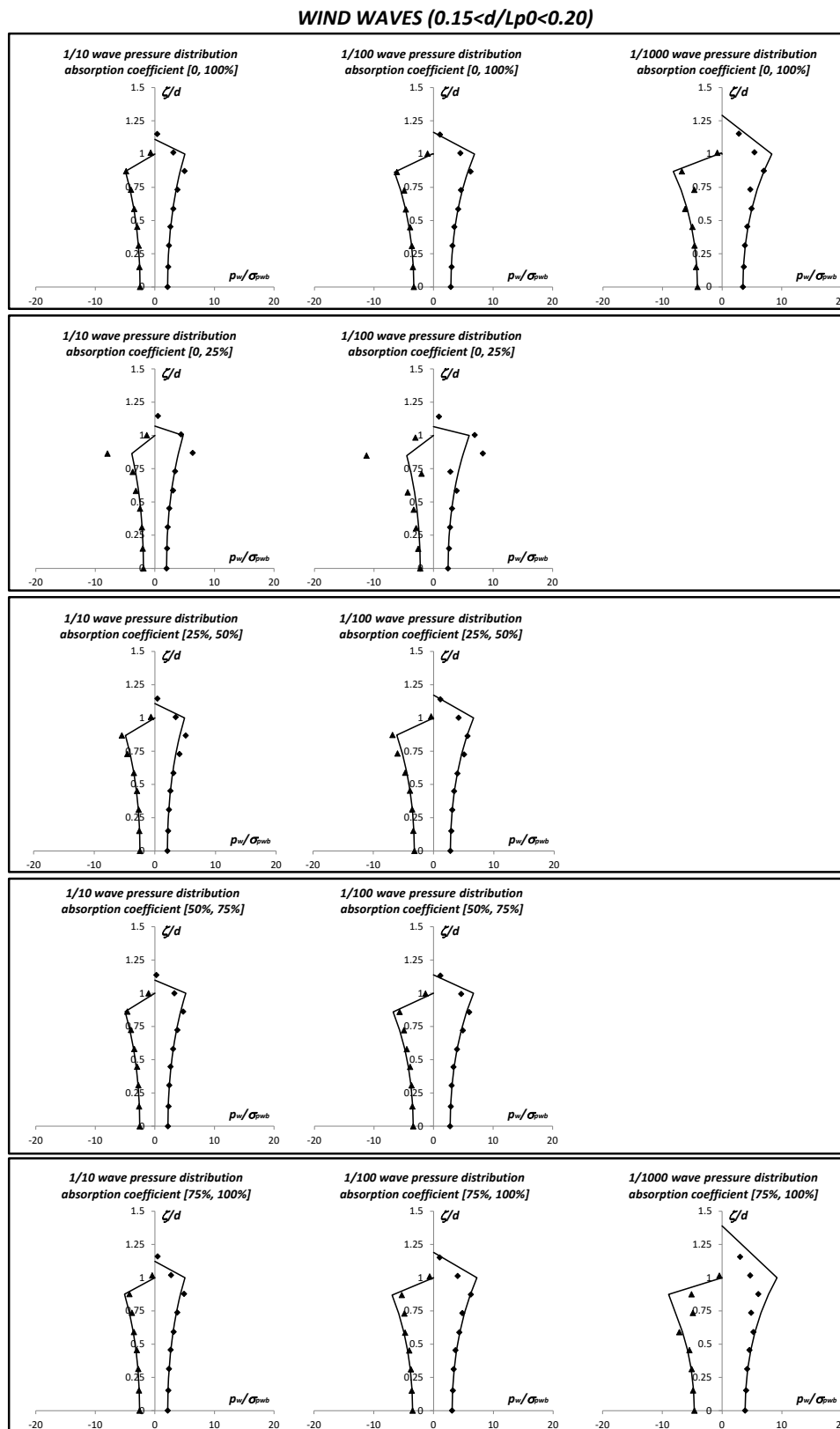


Figure 10. Average of the highest 1/10, 1/100 and 1/1000 wave pressure distribution (crests and troughs) of sea states constituted by wind waves in the fixed interval $[0.15, 0.20]$ of d/L_{p0} , for four classes of the absorption coefficient, ranging from 0% to 100%. Points are obtained by means of the experimental measures taken on the front wall of the U-OWC. The continuous lines are obtained by means of the linear wave theory.

10. Conclusions

The aim of this work is verifying the applicability of two wave pressure formulas to predict wave loads on a caisson breakwater embodying an OWC device. For that, an experiment at sea on the eastern coast of the Strait of Messina (Southern Italy) was carried out to determine the horizontal wave forces on the front wall of a 1:10 scale model of a U-OWC. A set of 774 sea states composed by pure wind generated waves (with average peak period of 2.5 s) were recorded, and results were compared with Goda's and Boccotti's formulas.

The average of the pressure distributions produced by the $n/10$, $n/100$ and $n/1000$ highest crests and by the $n/10$, $n/100$ and $n/1000$ deepest troughs of the horizontal force process (n = number of waves) was represented for fixed intervals of d/L_{p0} and sea state characteristics. To evaluate the effect of the energy absorbed by the U-OWC on the horizontal force produced by waves on the breakwater, four classes, from 0% to 100%, of the absorption coefficient (=mean captured energy flux/mean incident wave flux), are considered for each d/L_{p0} interval.

The energy absorption affects positively the wave pressure distribution on the wave-beaten wall of the breakwater. Indeed, the greater the absorption is, the more the wave pressure drops near the upper opening of the vertical duct. Consequently, the horizontal wave forces on the absorber breakwater are smaller than the horizontal forces on a conventional upright breakwater. This statement emerges comparing the results of the present field experiment with those of Boccotti et al. (2012) [14], using Goda's [1] and Boccotti's formulas [13] as a benchmark. Both the models predict extreme positive force peaks on a U-OWC breakwater with an appropriate safety factor. The underestimation of the negative force peaks by means of Boccotti's model is less than 7%.

By comparing the 1/1000 distribution of positive peaks of the force process, we have found that the linear wave theory overestimates the horizontal wave forces on the front wall of the REWEC3 by an average about 23%. Goda's formula overestimates them by an average about 28%. The same results have been obtained for the overturning moment. Actual and theoretical uplift forces are instead identical. In summary, the horizontal forces measured at sea are smaller than those predicted starting from the wave pressure formulas. The pressure distributions on the breakwater wall is strongly influenced by the energy absorbed by plant, which depends in its turn on the geometry of the plant and the wave characteristics (period and steepness). For this reason, improving the wave pressure formulas to evaluate the actual loads on the structure is very difficult. Therefore, despite this overestimation, we can conclude that both these models can be effectively used for the preliminary design stage of a U-OWC breakwater. Indeed, when performing a more accurate overall stability analysis of the breakwaters, it is necessary to consider also the hydrodynamics inside the plant (see [29]).

Our results are strategic also to implement adequate control strategies of the wave energy absorber. For example, a clear result of the field experiment is that the more the plant absorbs the less the horizontal force is. Indeed, the Boccotti's model underestimates by about 7% the actual wave force when the turbine duct is closed, and no air is exchanged with the atmosphere. On the contrary, a 27% overestimation of the actual horizontal force for 1/1000 distribution and $75\% < C_A < 100\%$ is found. This implies the necessity to design opportunely an exhaust tube to open when the turbine is not operating, in order to reduce the wave pressure both on the beaten wall and inside the plenum chamber. The sectional area of this tube must be large enough to let the plant to absorb a significant share of energy but, at the same time, not too large to permit the rising water to hit the caisson roof, producing a shock pressure.

Author Contributions: P.G.F.F. cured the conceptualization of the work and executed the field experiment. L.G. analized the experimental data, cured the methodology and data validation and prepared the original draft; P.G.F.F. reviewed the writing and supervised the work. All authors have read and agreed to the published version of the manuscript.

Funding: This research was funded by Consortium Okeanos.

Conflicts of Interest: The authors declare no conflict of interest.

Abbreviations

OWC	Oscillating Water Column
POS	Pieces Of Spectrum
REWEC1	Resonant Wave Energy Converter realization n.1
REWEC3	Resonant Wave Energy Converter realization n.3
U-OWC	U-shaped Oscillating Water Column

Nomenclature

The following symbols are used in this paper:

C_A	absorption coefficient;
C_D	diffraction coefficient;
\bar{C}_D	mean diffraction coefficient;
d	water depth;
d	depth above the armour layer of the rubble foundation in Goda's model;
E_u	energy spectrum in the undisturbed wave field;
E_w	energy spectrum in front of the U-OWC breakwater;
F	horizontal wave force per unit length on a section of a breakwater;
\tilde{F}	ratio between F and σ_F ;
$F_{1/N}$	average of the highest $N/1000$ peaks of the process $F(t)$;
$F_{B1/N}$	$F_{1/N}$ according to Boccotti's model;
F_G	wave force according to Goda's model;
f	frequency;
g	acceleration of gravity;
$H^{(+)}$	virtual wave height under a crest in Boccotti's model;
$H^{(-)}$	virtual wave height under a trough in Boccotti's model;
H_{max}	maximum wave height in Goda's model;
H_s	significant wave height of the incident waves;
$H_{1/3}$	mean wave height of the 1/3 largest waves in the sea state;
h	water depth in front of the upright breakwater in Goda's model;
h'	distance between the design water level and the bottom of the upright section in Goda's model;
h_b	water depth at a distance $5H_{1/3}$ seaward of the breakwater;
h_c	crest elevation of the breakwater above the still water level in Goda's model;
k	wave number;
L	wave length;
L_{p0}	dominant wave length in deep water;
n	number of waves;
p_{st}	hydrostatic pressure;
p_u	uplift pressure;
p_w	wave pressure;
$p_{wb}^{(+)}$	wave pressure at the lowest point of the front wall, at the instant of the wave crest;
$p_{wb}^{(-)}$	wave pressure at the lowest point of the front wall, at the instant of the wave trough;
p_1	wave pressure at the still water level in Goda's formula;
p_2	wave pressure at the bottom depth in Goda's formula;
p_3	wave pressure at the depth of the base of the armour layer in Goda's formula;
p_4	wave pressure at the structure crest in Goda's formula;
T_h	period of the highest waves;
T_p	peak period;
$T_{1/3}$	mean period of the 1/3 largest waves in the sea state;
t	time;

$\alpha_1, \alpha_2, \alpha_3$	coefficients in Goda's formula;
β	amplification factor of the wave amplitude at the U-OWC breakwater;
Δ_G	percent difference between Goda's model wave force and the actual value of $F_{1/1000}$;
$\Delta_{B1/N}$	percent difference between $F_{1/N}$ of Boccotti's model and the actual value of $F_{1/N}$;
$\lambda_1, \lambda_2, \lambda_3$	factors in Goda's formula;
ξ	vertical axis with origin at the base of the wall;
η^*	maximum wave elevation in the breakwater center;
ρ	water density;
θ	angle between the direction of the wave and the line normal to the breakwater;
θ_m	average θ in a sea state;
σ	standard deviation of the surface wave in the undisturbed wave field;
σ_F	standard deviation of the stationary random process $F(t)$;
σ_{pwb}	standard deviation of the wave pressure at the base of the wall;
ψ^*	narrow-bandedness parameter;
Φ_{abs}	instantaneous wave energy flux absorbed by the plant;
Φ_{in}	instantaneous energy flux of waves in the undisturbed field;
$\overline{\Phi}_{abs}$	time-averaged wave energy flux absorbed by the plant;
$\overline{\Phi}_{in}$	time-averaged energy flux of waves in the undisturbed field.

References

1. Goda, Y. Random seas and design of maritime structures. In *Advanced Series on Ocean Engineering*; World Scientific: Singapore, 2010; Volume 33.
2. Goda, Y.; Takagi, H. A reliability design method of caisson breakwaters with optimal wave heights. *Coast. Eng. J.* **2000**, *42*, 357–387. [[CrossRef](#)]
3. Oumeraci, H.; Kortenhaus, A.; Allsop, W.; de Groot, M.; Crouch, R.; Vrijling, H.; Voortman, H. *Probabilistic Design Tools for Vertical Breakwaters*; CRC Press: Boca Raton, FL, USA, 2001; ISBN 90-5809-249-6.
4. U.S. Army Corps of Engineers. *Coastal Engineering Manual—Part VI (CEM), Engineer Manual 1110-2-1100*; U.S. Army Corps of Engineers: Washington, DC, USA, 2002.
5. Sainflou, G. Essai sur les digues maritimes verticales. *Annales Ponts et Chaussées* **1928**, *98*, 4.
6. Hiroi, I. On a method of estimating the force of waves. *Mem. Engrg. Fac. Imp. Univ. Tokyo* **1919**, *X*, 19.
7. Minikin, R. *Wind, Waves and Marine Structures 2*; Charles Griffin: London, UK, 1950; pp. 38–39.
8. Ito, Y.; Fujishima, M.; Kitatani, T. On the stability of breakwaters. *Coast. Eng. Jpn.* **1971**, *14*, 53–61. [[CrossRef](#)]
9. Goda, Y. A new method of wave pressure calculation for the design of composite breakwater. In Proceedings of the Fourteenth Conference on Coastal Engineering, Copenhagen, Denmark, 24–28 June 1974; pp. 1702–1720.
10. Goda, Y. The design of upright breakwater. In Proceedings of the 23rd International Conference on Coastal Engineering, Venice, Italy, 4–9 October 1992; pp. 547–568.
11. Goda, Y. Dynamic response of upright breakwaters to impulsive breaking wave forces. *Coast. Eng.* **1994**, *22*, 135–158. [[CrossRef](#)]
12. Takahashi, S.; Tanimoto, K.; Shimosako, K. A proposal of impulsive pressure coefficient for the design of composite breakwaters. In Proceedings of the International Conference on Hydro-Technical Engineering for Port and Harbor Construction, Port and harbor Research Institute, Yokosuka, Japan, 19–21 October 1994; pp. 489–504.
13. Boccotti, P. *Wave Mechanics for Ocean Engineering*; Elsevier Science: Oxford, UK, 2000.
14. Boccotti, P.; Arena, F.; Fiamma, V.; Romolo, A.; Barbaro, G. Small-Scale Field Experiment on Wave Forces on Upright Breakwaters. *J. Waterw. Port Coast. Ocean Eng. ASCE* **2012**, *138*, 97–114. [[CrossRef](#)]
15. Boccotti, P. On a new wave energy absorber. *Ocean Eng.* **2003**, *30*, 1191–2000. [[CrossRef](#)]
16. Boccotti, P. Caisson breakwaters embodying an OWC with a small opening—Part I: Theory. *Ocean Eng.* **2007**, *34*, 806–819. [[CrossRef](#)]
17. Boccotti, P.; Filianoti, P.; Fiamma, P.; Arena, F. Caisson breakwaters embodying an OWC with a small opening—Part II: A small-scale field experiment. *Ocean Eng.* **2007**, *34*, 820–841. [[CrossRef](#)]
18. Filianoti, P.; Camporeale, S. A small scale field experiment on a wells turbine model. In Proceedings of the 7th European Wave and Tidal Energy Conference, Porto, Portugal, 11–14 September 2007.

19. Filianoti, P.; Camporeale, S. A linearized model for estimating the performance of submerged resonant wave energy converters. *Renew. Energy* **2008**, *33*, 631–641. [[CrossRef](#)]
20. Filianoti, P.; Piscopo, R. Sea wave energy transmission behind submerged absorber caissons. *Ocean Eng.* **2015**, *93*, 107–117. [[CrossRef](#)]
21. Arena, F.; Filianoti, P. Small-scale field experiment on a submerged breakwater for absorbing wave energy. *J. Waterw. Port Coast. Ocean Eng.* **2007**, *133*, 2. [[CrossRef](#)]
22. Sarmiento, A.J.; Falcao, A.F. Wave generation by an oscillating surface pressure and its application in wave-energy extraction. *J. Fluid Mech.* **1985**, *150*, 467. [[CrossRef](#)]
23. Raghunathan, S. The Wells turbine for wave energy conversion. *Prog. Aerosp. Sci.* **1995**, *31*, 335–386. [[CrossRef](#)]
24. Falcão, A.F.D.; Henriques, J.C.C. Oscillating-water-column wave energy converters and air turbines: A review. *Renew. Energy* **2016**, *85*, 1391–1424.
25. Torre-Enciso, Y.; Ortubia, I.; de Aguilera, L.I.L.; Marqués, J. Mutriku wave power plant: from the thinking out to the reality. In Proceedings of the 8th European Wave Tidal Energy Conference, Uppsala, Sweden, 7–10 September 2009; pp. 319–329.
26. Arena, F.; Fiamma, V.; Laface, V.; Malara, G.; Romolo, A.; Strati, F.M. Monitoring of the U-OWC under construction in Civitavecchia (Rome, Italy). In Proceedings of the 11th European Wave and Tidal Energy Conference, Nantes, France, 6–11 September 2015.
27. Boccotti, P. Design of breakwater for conversion of wave energy into electrical energy. *Ocean Eng.* **2012**, *51*, 106–118. [[CrossRef](#)]
28. Graw, K.U. Wave energy breakwaters—A device comparison. In Proceedings of the Conference in Ocean Engineering—coe'96, Madras, India, 17–20 December 1996.
29. Boccotti, P. *Wave Mechanics and Wave Loads on Marine Structure*; Butterworth-Heinemann: Amsterdam, The Netherlands; Boston, MA, USA, 2015.
30. Kuo, Y.-S.; Lin, C.-S.; Chung, C.-Y.; Wang, Y.-K. Wave loading distribution of oscillating water column caisson breakwaters under non-breaking wave forces. *J. Mar. Sci. Technol.* **2015**, *23*, 78–87.
31. Ashlin, S.J.; Sundar, V.; Sannasiraj, S.A. Pressures and forces on an oscillating water column-type wave energy caisson breakwater. *J. Waterw. Port Coast. Ocean Eng.* **2017**, *143*, 04017020. [[CrossRef](#)]
32. Ashlin, S.J.; Sannasiraj, S.A.; Sundar, V. Wave Forces on an Oscillating Water 506 Column Device. *Procedia Eng.* **2015**, *116*, 1019–1026. [[CrossRef](#)]
33. Filianoti, P. Pulsating flow discharge measurements inside a wave energy converter at sea. In Proceedings of the 6th IMEKO TC19 Symposium on Environmental Instrumentation and Measurements, Reggio Calabria, Italy, 24–25 June 2016.
34. Gurnari, L.; Filianoti, P.; Torresi, M.; Camporeale, S. The Wave-to-Wire Energy Conversion Process for a Fixed U-OWC Device. *Energies* **2020**, *13*, 283. [[CrossRef](#)]

